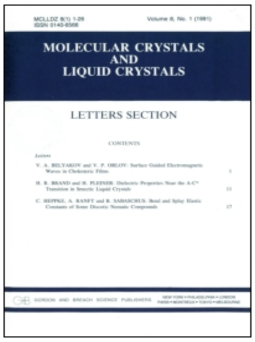

MOLECULAR CRYSTALS
AND
LIQUID CRYSTALS

LETTERS SECTION

Molecular Crystals and Liquid Crystals

ISSN: 1542-1406 (Print) 1563-5287 (Online) Journal homepage: http://www.tandfonline.com/loi/gmcl20

Growing poly(methyl methacrylate) chains from the surface of zinc oxide nanoparticles via surface-initiated reversible addition-fragmentation chain transfer polymerization

Long Giang Bach, Bui Thi Phuong Quynh & Kwon Taek Lim

To cite this article: Long Giang Bach, Bui Thi Phuong Quynh & Kwon Taek Lim (2016) Growing poly(methyl methacrylate) chains from the surface of zinc oxide nanoparticles via surface-initiated reversible addition-fragmentation chain transfer polymerization, Molecular Crystals and Liquid Crystals, 635:1, 12-17, DOI: 10.1080/15421406.2016.1200403

To link to this article: http://dx.doi.org/10.1080/15421406.2016.1200403

MOLECULAR CRYSTALS AND LIQUID CRYSTALS
2016, VOL. 635, 12–17
http://dx.doi.org/10.1080/15421406.2016.1200403

Growing poly(methyl methacrylate) chains from the surface of zinc oxide nanoparticles via surface-initiated reversible addition-fragmentation chain transfer polymerization

Long Giang Bach[a], Bui Thi Phuong Quynh[a], and Kwon Taek Lim[b]

[a]NTT Institute of Hi-Technology, Nguyen Tat Thanh University, Ho Chi Minh City, Vietnam; [b]Department of Imaging System Engineering, Pukyong National University, Busan, Korea

ABSTRACT
In the present work, we focus on fabrication of the novel nanocomposite, ZnO grafted with poly(methyl methacrylate) (PMMA), via surface-initiated reversible addition-fragmentation chain transfer (RAFT) polymerization. A trithiocarbonate RAFT agent was anchored onto ZnO nanoparticles in a simple procedure using a ligand exchange reaction of S-benzyl S′-trimethoxysilylpropyltrithiocarbonate (BTPT) with hydroxyl groups on the surface of ZnO nanoparticles. BTPT-anchored ZnO nanoparticles were then used for surface-initiated RAFT polymerization of MMA to fabricate structurally well-defined ZnO-g-PMMA hybrid nanoparticles. The structure, property and morphology of PMMA-g-ZnO nanocomposites were investigated by fourier transformed infrared spectroscopy (FT-IR), energy dispersive X-Ray (EDX), X-ray diffraction (XRD), thermogravimetric analysis (TGA) and field emission scanning electronic microscopy (FE-SEM)

KEYWORDS
ZnO nanoparticles; Poly(methyl methacrylate); PMMA-*g*-ZnO; RAFT polymerization

1. Introduction

Semiconductor nanocrystals have attracted a great deal of attention due to their unique size dependent optoelectronic properties [1, 2]. Compared to other II–VI compound semiconductors, ZnO possesses a wide band-gap of 3.37 eV and rather large exciton binding energy, which contribute to its stable exciton state even at room temperature [3]. An upsurge in research and development of the nanoscale ZnO over the past decade has brought about a vast area of new potential applications such as light-emitting diodes, photodetectors, field-effect transistors, sensors, transducers, nanocantilevers, thermal transport elements and new types of solar cells [4–6]. Furthermore, the environmentally friendly property of ZnO makes it a desirable material for bio-applications like bio-imaging and cancer detection. However, as a class of nanomaterials, ZnO nanoparticles are vulnerable to agglomeration due to their high surface energy particularly when dispersed in organic solvent and matrices thus leading to significant loss in desired activities. Thereafter, the drawbacks of using ZnO nanostructured materials can be overcome by preparing ZnO-polymer nanocomposites to embed a relatively small content of inorganic nanoparticles [7–9]. Moreover, the inorganic core/organic shell hybrid composite

---

CONTACT Long Giang Bach ✉ blgiangntt@gmail.com 🖃 NTT Institute of Hi-Technology (NIH), Nguyen Tat Thanh University, Ho Chi Minh City, Vietnam.
Color versions of one or more of the figures in the article can be found online at www.tandfonline.com/gmcl.

nanoparticles possess unique optical, mechanical, thermal and electrical properties that are associated with broad application perspectives on large scale [10, 11].

Tethering of polymer brushes on a solid substrate has emerged as an effective method to modify the surface properties. The “living”/controlled radical polymerization techniques such as ATRP, MNP and RAFT offer densely packed array of polymer chains and are playing an increasingly important role in polymeric functionalization of inorganic nanoparticles [12–14]. Especially, RAFT polymerization has become one of the most promising controlled radical polymerization techniques to prepare polymer grafted solid supports, due to its tolerance to a wide range of reaction conditions, straightforward setup to result in block copolymers, and versatility towards a wide range of monomers with variable functionalities [15, 16]

Based on the aforementioned background, development of a facile chemical strategy to deliver ZnO based nanocomposites with suitable processability and dispersibility has been still unmet demand. Our strategy is to modify the inorganic ZnO surface by a one-step direct anchoring of the RAFT moiety. Subsequent grafting polymerization of MMA from ZnO-RAFT surface was conducted to afford PMMA-*g*-ZnO nanocomposites.

2. Experimental

Materials

Methyl methacrylate (MMA) was purified by passing the liquid through a neutral alumina column to remove inhibitors. 2,2′-Azobisisobutyronitrile (AIBN) was recrystallized from methanol before use. (3-mercaptopropyl) trimethoxysilane (MPTMS, 95%), sodium methoxide (95%), carbon disulfide (CS2) (99.9%), benzyl bromide (98%), ZnO nanoparticles and all solvents were used as received. All of the above chemicals were purchased from Sigma-Aldrich.

Modification of ZnO nanoparticles with RAFT agent

The synthesis of S-benzyl S-trimethoxysilylpropyltrithiocarbonate (BTPT) as RAFT agent was conducted according to the procedure described in the previous study [18]. Immobilization of the RAFT agent on the ZnO NPs surface was conducted as follows. The ZnO nanoparticles (2g) were first dispersed in methanol (50 ml) in a 100 ml round flask followed by the addition of BTPT (0.5 g). The mixture was further dispersed for 20 min through ultrasonication at room temperature before being heated to reflux for 6 h. At the end of the reaction, the mixture was cooled down and washed with excess THF, and dried under vacuum at room temperature overnight.

Synthesis of PMMA-g-ZnO nanocomposites via surface-initiated RAFT polymerization

To a 50 mL round flask, equipped with a Teflon-coated magnetic bar and a reflux condenser, was added MMA (2g), ZnO-RAFT (0.2g) and AIBN (1.2 mg) in 4 mL of THF. The flask was purged with N_2, heated to 90 °C and kept stirring for 12h. After polymerization, the flask was cooled to room temperature and the reaction mixture was precipitated in methanol before being filtered and dried in a vacuum oven. Next, the polymer product was diluted in toluene and centrifuged to collect the PMMA-*g*-ZnO free from the unbound polymer.

Scheme 1. Covalent modification of ZnO by PMMA via SI-RAFT polymerization.

Characterization

Fourier-transformed infrared (FT-IR) spectra were recorded to characterize the chemical changes in the surface functionalities of ZnO using a BOMEM Hartman & Braun FT-IR spectrometer. GPC was performed using an Agilent 1200 Series equipped with PLgel 5 μm MIXED-C columns, with tetrahydrofuran as the solvent and calibration was carried out using PS standards. The differential scanning calorimetry (DSC) measurements were conducted using a Perkin Elmer calorimeter (DSC6200). Thermogravimetric analysis (TGA) was conducted with Perkin-Elmer Pyris 1 analyzer (USA). The morphology and elemental analysis of the hybrids were carried out by using Field Emission Scanning Electron Microscopy (FE-SEM) images equipped with an Energy Dispersive X-Ray (EDX) spectrometer (Hitachi JEOL-JSM-6700F system, Japan).

3. Results and discussion

A schematic representation for the preparation of PMMA-*g*-ZnO nanocomposites is illustrated in Scheme 1. The ZnO-RAFT was first prepared by treating ZnO nanoparticles with BTPT followed by surface initiated radical polymerization of MMA from ZnO-RAFT nanoparticles.

FT-IR was used to investigate the bonding nature in the prepared nanocomposites. Fig. 1 shows the FT-IR spectra of ZnO nanoparticles, ZnO-RAFT and PMMA-*g*-ZnO nanocomposites. For ZnO nanoparticles (Fig. 1A), the band at 498 cm^{-1} is the characteristic absorption of Zn–O bond and the broad absorption band at 3427 cm^{-1} can be attributed to the absorption of hydroxyl groups. The introduction of RAFT agent to ZnO NPs surface was confirmed by Fig. 1B which exhibits the FT-IR absorption peaks of CH_2- moieties at 2926 and 2843 cm^{-1} and a weak but visible band at 3055 cm^{-1} assigning for sp^2 C-H stretching of aromatic ring. Ring stretch absorption of the RAFT agent appeared at 1651 and 1487 cm^{-1}, indicating that the RAFT agent was immobilized onto the surface of the ZnO nanoparticles *via* the silane coupling reaction [17]. In the FT-IR spectrum of the PMMA-*g*-ZnO (Fig. 1C), a new adsorption band at 1722cm^{-1} indicating the presence of C=O stretching vibration of PMMA and the bands in the range of 3000 - 2850cm^{-1} corresponding to the C–H stretching vibrations of the CH_3 and CH_2 groups of grafted PMMA were observed. Therefore, it can be concluded that PMMA was covalently grafted onto the surface of ZnO nanoparticles.

Furthermore, the anchoring of RAFT agent and growing PMMA chains from ZnO NPs surface via surface-initiated RAFT polymerization was further verified by EDX analysis. The characteristic peaks ascribed to C, Zn and O elements appeared in the EDX spectrum of ZnO

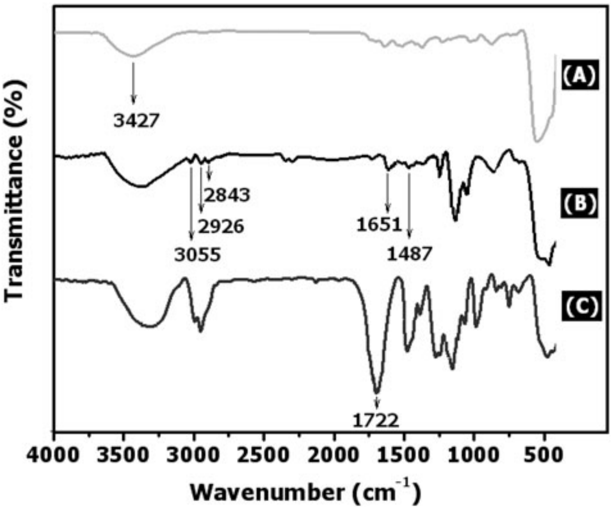

Figure 1. FT-IR spectra of (A) ZnO nanoparticles, (B) ZnO-RAFT and (C) PMMA-*g*-ZnO nanocomposites.

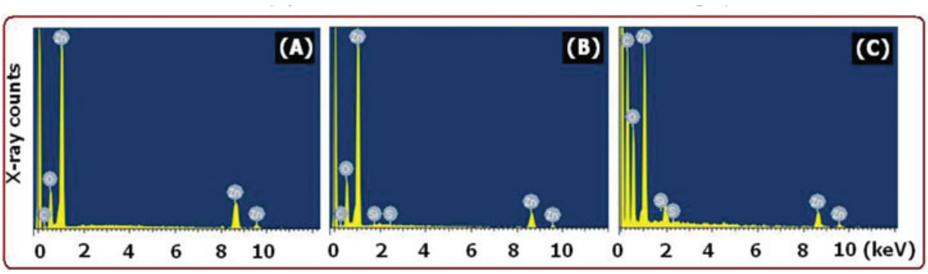

Figure 2. EDX analysis of (A) ZnO nanoparticles, (B) ZnO-RAFT and (C) PMMA-*g*-ZnO nanocomposites.

NPs (Fig. 2A). The EDX spectrum of ZnO-RAFT (Fig. 2B) reveals small but detectable peaks of Si and S atoms available on the NPs surfaces, indicating the anchoring of RAFT agent on the ZnO surface. In case of the PMMA-g-ZnO nanocomposite, the peaks corresponding to C, O, Zn, S, and Si elements were detected (Fig. 2C). These results indicate that PMMA chains were successfully grafted from the surface of ZnO NPs *via* RAFT polymerization.

The morphologies of ZnO nanoparticles, ZnO-RAFT and PMMA-*g*-ZnO nanocomposites were characterized by FE-SEM analysis. As can be seen in Fig. 3A vs Fig. 3B, the structure of ZnO-RAFT is almost identical with that of the needle-like ZnO nanoparticles. After polymerization, change in morphology of ZnO nanoparticles due to the grafting of PMMA brushes

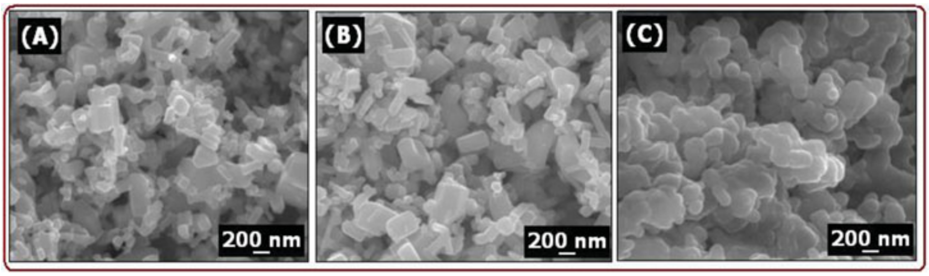

Figure 3. FE- SEM images of (A) ZnO nanoparticles, (B) ZnO-RAFT and (C) PMMA-*g*-ZnO nanocomposites.

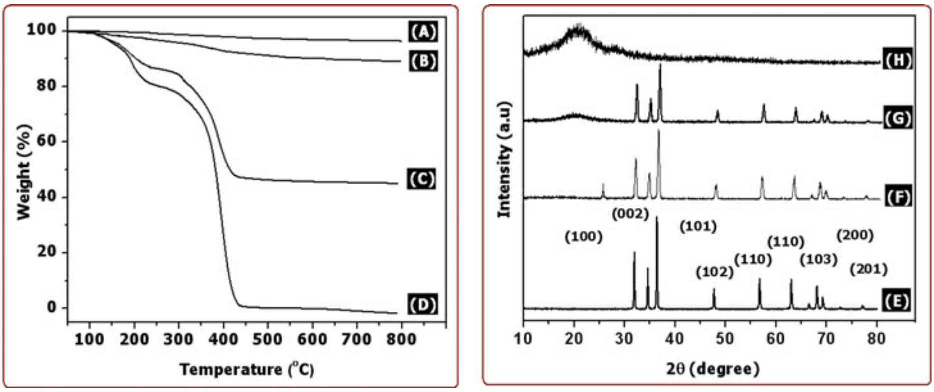

Figure 4. TGA scans of (A) ZnO nanoparticles, (B) ZnO-RAFT, (C) PMMA-*g*-ZnO nanocomposites and (D) polymer PMMA; XRD patterns of (E) ZnO nanoparticles, (F) ZnO-RAFT, (G) PMMA-*g*-ZnO nanocomposites and (H) polymer PMMA.

on the particle surface was found as revealed by Fig. 3C. Accordingly, it is suggested that the crystals of ZnO nanoparticles were embedded by PMMA chains.

To study the thermal behavior and the amount of PMMA grafted onto ZNO NPs, TGA studies of the samples were undertaken (Fig. 4A–D). The pristine ZnO NPs showed a weight loss of *ca.* 4.8%, while heated from 50 to 800°C due to the elimination of physically and chemically adsorbed water and the decomposition of hydroxide groups available on the surface of ZnO NPs (Fig. 4A). The RAFT agent modified ZnO NPs (Fig. 4B) showed a weight loss of *ca.* 11.2%, thus, the content of the coupling RAFT agent grafted onto the surface of ZnO NPs was estimated to be *ca.* 6.4 wt%. In comparison with the pristine ZnO NPs and ZnO-RAFT, the total weight loss of PMMA-*g*-ZnO nanocomposites as shown in Fig. 4C was much higher, presumably due to the presence of a significant amount of PMMA polymer which was decomposed completely at ca. 400 °C (Fig. 4D). Accordingly, the degree of grafting of PMMA onto ZnO NPs was calculated to be 43.5%.

To check the effect of grafting polymerization on the crystalline structure of ZnO nanoparticles, X-ray powder diffraction (XRD) patterns of ZnO nanoparticles before and after PMMA grafting were recorded as demonstrated in Fig. 4H–E. As can be seen in XRD patterns of the as prepared ZnO NPs, all of the diffraction peaks could be indexed to pure wurtzite phase of ZnO [3]. Note that the characteristic peaks of PMMA-*g*-ZnO nanocomposites almost resembled those of ZnO nanoparticles with an additional signal of the grafted PMMA in the 2θ range of 20–25°, suggesting that the grafting polymerization did not alter the crystalline structure of ZnO nanoparticles. Moreover, the presence of PMMA resulted in a decrease of the crystallite size represented by less sharp diffraction peaks.

4. Conclusions

In this study, a facile, efficient surface initiated controlled polymerization approach to prepare chemically bonded PMMA-*g*-ZnO nanocomposites via SI-RAFT polymerization has been unlocked. The results of FT-IR and EDS analyses revealed that the surface of ZnO nanoparticles were successfully grafted with PMMA *via* the covalent linkage between ZnO and polymer. The crystallinity of ZnO nanostructure, as characterized via XRD patterns, did not change upon the grafting of PMMA. Additionally, TGA results indicated an enhancement of thermal stability of PMMA-g-ZnO nanocomposites compared to pure PMMA polymer. Above all, this versatile approach can be applied to graft other polymers with increasing complexity and functionality in the polymeric shells and may pave the way for novel design, fabrication, optimization, and eventual application of other functional ZnO related nanocomposites.

Acknowledgments

This research is funded by Vietnam National Foundation for Science and Technology Development (NAFOSTED) under grant number 104.02–2014.53. Authors would like to thank Nguyen Thi Thuong, Xuan Thang Cao, Cam Anh Thieu, Thanh Khoa Phung, Giang Ngoc Ha, Van Thuan Tran from Nguyen Tat Thanh University, Ho Chi Minh City, Vietnam for the synthesis of S-benzyl S-trimethoxysilylpropyltrithiocarbonate.

References

[1] Bach, L.G. et al. (2013). *Appl. Surf. Sci.*, *283*, 546.
[2] Saravanan, R. et al. (2015). *J. Colloid Inter. Sci.*, *452*, 126.
[3] Peng, X. et al. (2009). *Appl. Surf. Sci.*, *255*, 7158.
[4] Liu, W. et al. (2014). *Mol. Cryst. Liq. Cryst.*, *603*, 216.
[5] Choi, S.C. et al. (2014). *Mol. Cryst. Liq. Cryst.*, *602*, 72.
[6] Zhou, H. et al. (2015). *J. Colloid Inter. Sci.*, *448*, 367.
[7] Sato, M. et al. (2008). *Eur. Polym. J.* 44, 3430.
[8] Kulyk, B. et al. (2010). *J. Alloys Compd.*, *502*, 24.
[9] Abdolmaleki, A. et al. (2011). *Appl. Surf. Sci.*, *257*, 6725.
[10] Spitalsky, Z.el al. (2010). *Prog. Polym. Sci.*, *35*, 357.
[11] Oh, J.K. et al. (2011). *Prog. Polym. Sci.*, *36*, 168.
[12] Matyjaszewski, K (2012). *Macromolecules*, *45*, 4015.
[13] Keddie, D.J. et al. (2012). *Macromolecules*, *45*, 5321.
[14] Braunecker, W.A.el al. (2007). *Prog. Polym. Sci.*, *32*, 93.
[15] Beija, M. et al. (2011). *Prog. Polym. Sci.*, *36*, 845.
[16] Rozenberg, B.A. et al. *(2008) Prog. Polym. Sci.*, *33*, 40.
[17] Cao, X.T. et al. (2014). *Mol. Cryst. Liq. Cryst.*, *599*, 55.